Model for the Findings about Hologram Generating Properties of DNA

P. Gariaev, gariaev@mail.ru
and
M. Pitkänen, matpitka@uukku.com.
http://tgd.wippiespace.com/public_html/.

December 11, 2010

Abstract

A TGD inspired model for the strange replica structures observed when DNA sample is radiated by red, IR, and UV light using two methods by Peter Gariaev and collaborators. The first method produces what is tentatively interpreted as replica images of either DNA sample or of five red lamps used to irradiate the sample. Second method produce replica image of environment with replication in horizontal direction but only at the right hand side of the apparatus. Also a white phantom variant of the replica trajectory observed in the first experiment is observed and has in vertical direction the size scale of the apparatus.

The model is developed in order to explain the characteric features of the replica patterns. The basic notions are magnetic body, massless extremal (topological light ray), the existence of Bose-Einstein condensats of Cooper pairs at magnetic flux tubes, and dark photons with large value of Planck constant for which macroscopic quantum coherence is possible. The hypothesis is that the first method makes part of the magnetic body of DNA sample visible whereas method II would produce replica hologram of environment using dark photons and produce also a phantom image of the magnetic tubes becoming visible by method I. Replicas would result as mirror hall effect in the sense that the dark photons would move back and forth between the part of magnetic body becoming visible by method I and serving as a mirror and the objects of environment serving also as mirrors. What is however required is that not only the outer boundaries of objects visible via ordinary reflection act as mirrors but also the parts of the outer boundary not usually visible perform mirror function so that an essentially 3-D vision providing information about the geometry of the entire object would be in question. Many-sheeted space-time allows this.

The presence of the hologram image for method II requires the self-sustainment of the reference beam only whereas the presence of phantom DNA image for method I requires the self-sustainment of both beams. Non-linear dynamics for the energy feed from DNA to the magnetic body could make possible self-sustainment for both beams simultaneously. Non-linear dynamics for beams themselves could allow for the self-sustainment of reference beam and/or reflected beam. The latter option is favored by data.

Contents

1 Introduction

The findings of Gariaev's group include the rotation of polarization plane of laser light by DNA [4], phantom DNA effect [3], the transformation of laser light to radio wave photons having biological effects [6], the coding of DNA sequences to the modulated polarization plane of laser light and the ability of this kind of light to induce gene expression in another organisms provided the modulated polarization pattern corresponds to an "address" characterizing the organism [4], and the formation of images of what is believed to be DNA sample itself and of the objects of environment by DNA sample in a cell irradiated by ordinary light in UV-IR range [5].

1.1 The notion of wave genome

Peter Gariaev and collaborators have introduced the notion of wave genome [4] requiring the coding of DNA sequences to temporal patterns of coherent em fields forming a bio-hologram representing geometric information about the organism. Code could mean that nucleotide is represented by a characteristic rotation angle for the polarization plane of linearly polarized laser radiation scattering from it. The experiments of Peter Gariaev's team [6] suggest that this kind rotation is induced by chromosomes by a mechanism which to my best knowledge is poorly understood. Other open questions concern the precise identification of the substrate of the bio-hologram, of the reference wave and of information carrying wave, and of the mechanism making possible (quantum) coherence in macroscopic length scales.

The reading of the DNA sequence to a radiation pattern is assumed to rely on the propagation of an acoustic soliton along DNA [4]. Whatever this process is, one should also identify the reverse process inducing the activation of the genome as the target organism receives the radiation coding for the DNA provided the genetic "address" is correct. One should also identify the mechanism transforming laser radiation to radio-waves at various frequencies as well as the mechanism creating what is believed to be the image of DNA sample and replicated images of some instruments used in experiment.

1.2 Hologram like radiation patterns generated by DNA

In this article one particular experiment, namely the already mentioned experiment involving the formation of two kinds of strange replica structures resulting when DNA sample is radiated by red, IR, and UV light using two methods by Gariaev's group [5] will be discussed. The original interpretation of the image produce by first method is as a replica image of DNA sample. This interpretation can be challenged. The second image is interpreted as a hologram image of the environment. In the following the interpretation of these images in TGD framework is discussed.

The first method produces what was originally interpreted as replica images of either DNA sample or of five red lamps used to irradiate the sample. Second method produce replica image of environment with replication in horizontal direction but only at the right hand side of the apparatus. Also a white phantom variant of the replica trajectory observed in the first experiment is observed and has in vertical dir

1.3 Basic TGD based notions involved with the model

In this article a model explaining the characteristic features of the replica patterns is developed. The model is inspired by Topological Geometrodynamics (TGD), the recent state of which is discussed in Prespacetime Journal [12]. TGD is a proposal for a unified theory of the fundamental interactions based on a generalization of the notion of space-time having perhaps its most important consequences at the level of living systems. TGD inspired theory of consciousness and of quantum biology is discussed in the articles [13, 14, 15] of Journal of Consciousness Research & Exploration. The model differs in many respects from the general model of proposed by Peter Gariaev and collaborators [4] but shares with it the vision about holograms as a basic element of information processing in living systems at DNA level.

The basic notions are magnetic body, massless extremal (topological light ray), the existence of Bose-Einstein condensates of Cooper pairs at magnetic flux tubes, and dark photons with large value of Planck constant for which macroscopic quantum coherence is possible. Also the hypothesis that the differences of zero point kinetic energies for space-time sheets with different p-adic length scales define universal metabolic energy quanta is used in the model for pumping of radiation energy to the system. The hypothesis is that the first method makes part of the magnetic body of DNA sample visible whereas method II would produce replica hologram of environment using dark photons and also the phantom image of the flux tubes becoming visible by method I.

Replicas would result by mirror hall effect in the sense that the dark photons would move back and forth between the part of magnetic body becoming visible by method I and serving as a mirror and the objects of environment serving also as mirrors. What is however required is that not only the outer boundaries of objects visible via ordinary reflection act as mirrors but also the parts of the outer boundary not usually visible perform mirror function so that an essentially 3-D vision providing information about the geometry of the entire object would be in question. Many-sheeted space-time allows this.

The presence of the hologram image for method II requires the self-sustainment of the reference beam only whereas the presence of phantom DNA image for method I requires the self-sustainment of both beams. Non-linear dynamics for the energy feed from DNA to the magnetic body could make possible self-sustainment for both beams simultaneously. Non-linear dynamics for beams themselves could allow for the self-sustainment of reference beam and/or reflected beam. The latter option is favored by data.

2 Observations

Two methods are involved to produce images with replica structure in the experiments of Gariaev's team. The detailed experimental arrangement and results of these experiments are described in [5]. Reader can get a concrete idea about the experiments from the figures at the end of this article.

For both methods one uses sources of red and IR photons emitted by diodes as well as sources of UV-B and UV-C photons (for a schematic representation of the experimental apparatus Fig. 13). The wave lengths and energies for red and IR photons are given by the following table.

$$\begin{array}{lll} \lambda/\mathrm{nm} & 650 & 920 \\ E/\mathrm{eV} & 1.91 & 1.35 \end{array} \tag{2.1}$$

The wave-length and energy intervals for UV-B and UB-C radiation are given by the following tables.

$$\begin{array}{lll} \text{Energy range} & [\lambda_1,\lambda_2]/\mathrm{nm} & [E_1,E_2]/\mathrm{eV} \\ UV-B & [315,280] & [3.94,4.43] \\ UV-C & [280,100]] & [4.43,12.40] \end{array} \tag{2.2}$$

1. In method I red, IR, and UV-B and UV-C beams are present all the time. During irradiation is one detects what are called DNA replica trajectories (Figs. 3 and 4) These roughly vertical tubular structures (or less probably, planar structures orthogonal to the preferred horizontal

direction) have grainy structure (Fig. 3). Replica trajectories decompose to five sub-trajectories which probably correspond to the five red diodes irradiating DNA directly (Fig. 4). One could interpret the replica trajectories as images of DNA sample or of red diodes created by the DNA sample.

Long-lived red DNA replica trajectories called phantom DNA trajectories are present also when the irradiation has ceased (Fig. 5). The distributions of brightness for these images in RGB model are represented in Fig. 6 representing especially clearly the structure of the trajectories.

2. In method II same beams are present but only periodically. The replicas appear when the beams are not on and are in horizontal direction representing environment (Fig. 2). The basic feature is that the objects of environment are replicated in horizontal direction with distance defined by the horizontal size of the object so that fractal structure results. There are also phantom DNA replicas which are white and to the left of DNA sample and could correspond to the red replicas seen by method I (Fig. 2). These structures are thicker than than the red replica trajectoriess of method I.

   What is remarkable that the replicas representing environment carry information about the geometry of the entire objects rather than that for the outer surface of these objects seen in reflection: a kind of 3-dimensional vision seems to be in question which cannot be explained in terms of ordinary holograms alone. The vertical region in which replicas are obtained corresponds to the height of the roughly vertical replica structures produced by method I.

   What is equally remarkable is that the replicas appear only at the right hand side of the system but not at the left hand side. Strangely, the touching of the DNA sample however shifts replicas to the left after which they disappear in about 5 to 8 seconds (Fig. s 7 and 8). The color of the replicas can be white, reddish, red and even blue. It is not quite clear whether the left replicas are mirror images of right replicas or images of the left hand side of the environment.

In both cases the key question is whether the replica trajectories represent real physical objects or whether they are analogous to a sequence of mirror images resulting when one has object between two mirrors and repeated reflections create a sequence of images replicas (mirror hall effect).

3 Model for the findings

The model for the findings is based on TGD inspired model of quantum biology. The key physical input of the TGD based model are the notions of magnetic body [30] and of massless extremal (ME) or topological light ray [27], and the identification of dark matter in terms of a hierarchy of Planck constants [23] assumed to play a key role in living matter. These notions are described briefly in [15]. A more detailed descriptions can be found in online books about TGD: for magnetic body in [30, 31], for MEs in [27] and for the hierarchy of Planck constants in [23].

3.1 Basic notions and ideas

The key notions and ideas of the TGD inspired model are the same as of the model discussed in [26] as a possible framework for understanding the findings of Gariaev's team. Only the treatment is considerably more detailed.

1. In TGD inspired theory of quantum biology one assigns to all biological structures magnetic bodies which use biological bodies as sensory receptors and motor instruments. This is assumed to hold true for DNA nucleotides, DNA strands, and even DNA sample itself so that an onion like hierarchy of magnetic bodies results. The basic vision is that magnetic flux sheets traversing through DNA integrate the DNAs of various nuclei to super DNA and that this occurs at level of organs, organisms and even populations and makes possible coherent gene expression responsible for the ability of living organisms to behave as single unit and also co-operate [24, 31]. The magnetic flux quanta and flux sheets can also end to the objects of the environment and this is essential for the model to be proposed.

   The matter at flux quanta is identified as dark matter and has Planck constant which is integer multiple of the ordinary one, and can be quite large so that macroscopic quantum coherence

becomes possible. This makes possible the formation of holograms and mirror hall effect since the dark counterparts of the ordinary photons can have wave length much longer than the size scale of the experimental apparatus.

Although the DNA preparation in the experiments of Gariaev's team is formed from a cellular structure by a violent chemical process removing proteins and cellular and nuclear membranes, the magnetic body of DNA sample could remain intact so that a natural hypothesis is that magnetic body are involved with the formation of both DNA replica trajectories and hologram like replica trajectories.

2. Topological light rays (MEs) are tubular structures very much analogous to laser beams. They carry radiation moving with light velocity and without dispersion and dissipation in single space-time direction that they are ideal for communication and control purposes. This linear superposition of only modes with parallel 4-D wave vectors is a key distinction from Maxwell's electrodynamics and due to non-linearity of the fundamental variational principle. More precisely, if one changes the direction of the 4-D wave vector opposite, both 3-D wave vector and frequency change sign so that the counterpart of phase conjugate laser light is in question. Hence one would have superpositions of beams and their phase conjugates having interpretation as positive and negative energy signals traversing in opposite spatial and temporal directions. At quantum level one might perhaps speak positive and negative energy photons.

   MEs could topologically condense at magnetic flux quanta and would be accompanied by the TGD counterparts of Alfven waves [17] representing transverse geometric oscillations of the magnetic flux quanta (sheets and tubes) regarded as space-time surfaces. It would be very natural to assume that topological light rays serve as correlates for the photons reflected from DNA sample to its magnetic body. In rather precise sense these photons would represent the scaled variant of EEG used by magnetic body to control brain and receive information from brain in TGD based model of brain.

3.2 Method I

The details of method I and the absence of the image of the environment (Fig. 3) in this case do not encourage hologram interpretation. The interpretation coming first in mind is that the DNA replica trajectory is realized at magnetic flux tubes serving as a screen. Flux sheets orthogonal to the plane of the images cannot be excluded but are less not plausible. The simplest assumption is that the photons of red light travel scattered from DNA sample to the magnetic flux tube like structures defining the screen along MEs topologically condensed at magnetic flux sheets traversing through DNA strands which are partially un-winded and have length of order 1 cm. Red light could transform to dark photons with large Planck constant with wavelength of order 1 cm but at the magnetic body it would transform partially back to visible photons. This is however not necessary. Also UV and IR photons would interact with the DNA sample and could provide the metabolic energy allowing also to amplify the signal. Also UV and IR photons could transform to dark photons and define part of the "EEG" of the DNA sample.

3.3 Method II

For method II the interpretation in terms of a hologram like structure resulting when light traveling in horizontal direction is reflected from the objects of the environment is suggestive.

1. For white cable like structures left from DNA sample referred to as phantom DNA replicas the grainy replica structure is actually not present (Fig. 2) so that phantom DNA replica is perhaps not the proper term. As in the case of method I these structures could be interpreted as images of the magnetic body serving as the hologram substrate. Since red light source is off, only the white light emitted by the DNA substrate is present. These structures are wider than the red DNA replicas and a rough estimate for their thickness is about 1 cm so that the interpretation as a flux tube of magnetic body is suggestive. The interpretation of the signal as counterparts of bio-photons [7] generated when dark photons transform to ordinary visible photons is suggestive.

2. Hologram interpretation for the replica of environment (Fig. 2) requires the system generates the reference beam prevailing for some time although the irradiations are turned off. The reflected

beams due to the irradiation would disappear as the irradiation is turned off so that the reference beam can generate the hologram image.

3. The simplest assumption is that there are horizontal flux tubes or sheet(s) in the plane defined by the vertical and horizontal directions and that the part of the magnetic body corresponding to DNA replica trajectory serves as source of dark photons with large $\hbar$ [23], which travel to the right in horizontal direction and along flux tubes connected to the outer surfaces of the objects of environment. If the dark photons emanate from the structures visible as phantom DNA replica, one can understand why the image is from the right hand side.

4. Similar connections to other living organisms would explain the original observations of Gurwitsch about mitogenic radiation at UV frequencies [16]: the UV radiation would represent decay products of dark variants of UV photons. One could also interpret bio-photons [7] at visible wavelengths as decay products of their dark variants with much longer wave lengths. These photons could produce also bunches of EEG photons for large enough value of $\hbar$ [31]. Also the findings of Gariaev's group about the transformation of laser light irradiating DNA to a radiation in a wide range of frequencies extending at least down to 10^4 Hz (corresponds to a wavelength of about 10 km) and having biological effects [6] could be interpreted in terms of long wave length dark photons with energies of visible photons. The role of low frequencies down to 10^4 Hz at least in water memory [8, 9] suggests that the basic mechanism of water memory is based on dark radio wave photons. The recent findings of the group led by HIV nobelist Jean-Luc Montagnier [10] relating to water memory suggest an interaction between DNA samples based on radiation and also a new non-chemical representation of genetic code in terms of electromagnetic radiation patterns proposed also by Gariaev's team [4, 6]. TGD approach suggests besides field representation based on MEs [29], a representation in terms of flux tubes connecting DNA and lipids of cell membrane [24], and a representation of genetic code in terms of the states of dark nucleons [25]. Computer science inspired view indeed suggests DNA provides only one of the many representations of the genetic code.

5. What differentiates the hologram from the ordinary one is that reflections occur from the entire outer surfaces- not only from the outer surface visible in ordinary sense but also from the "inner side" of the part not usually visible so that information about entire 3-D geometry is obtained (Fig. 2). Without this assumption it is difficult to understand the replication in the scale of the replicated object. The repeated travel back and forth along these flux tubes or sheets would produce mirror hall effect and the observed replica structure could be understood.

6. A possible reason for why replicas are horizontal is that the magnetic body of DNA sample receives information from the environment and the objects are of environment tend to be in the horizontal direction. Phantom DNA replicas which might relate to phantom DNA effect [3] discovered also by Gariaev's group appear only at the left hand side of the DNA sample and if they represent ordinary images of the hologram substrate and serve as mirrors, the appearance of the hologram replicas at the right hand side only can be understood. These images would result as dark photons emitted by the hologram substrate transforms to visible light.

   What happens in phantom DNA effect is that laser light scatters from the chamber weakly even after the DNA sample has been removed. The simplest explanation could be that some fraction of DNA leaves their magnetic bodies to the sample and that the scattering involves these magnetic bodies already in the original situation. Also water memory [8, 9, 10] could be due to the fact that for some fraction of the biological molecules originally present in the solution before dilution leaves the magnetic bodies in the sample and generate the radiation responsible for the biological effects as cyclotron radiation [29].

7. The hologram image would result as the photons of the reflected reference beam transform back to photons of visible (and possibly UV and IR) light. The reflection preserves only the vertical momentum of photon parallel to the flux tube so that reflections occur also in the direction of the camera. The photons in question need not correspond to single wave length. The UV radiation necessary for the experiment might serve as a metabolic energy source allowing to generate dark photons but it could also transform to dark photons defining the hologram. The longitudinal coherence length [11]

$$\xi = \frac{c}{\Delta f} = \frac{\lambda_d^2}{\Delta\lambda_d} = r\frac{\lambda^2}{\Delta\lambda} \quad , \quad r = \frac{\square}{\square_0}$$

of dark photons must be larger than the size scale L ~ 20 cm of the experimental apparatus in order to produce mirror hall effect. From the assumption that the size scale l ~ 1 cm of the grains of the replica trajectory is of order $l \sim r\lambda$, one obtains the estimate $r = 15 \times 2^{10}$. This gives $\lambda/\Delta\lambda \sim 20$, which looks rather reasonable value.

The transformation of the right-handed mirror hall image to left handed as the DNA sample is touched should be also understood.

1. The first question is whether the effect of touch (Figs. 7 and 8) is mechanical or biological. The proposed model encourages to consider the possibility that the magnetic body assignable to the hand or finger touching the sample generates the external irradiation generating dark photons needed to generate a replica hologram from the left hand side of the apparatus. When the finger is removed from the vicinity of the sample, one expects that the hologram disappears as it indeed does within 5-8 seconds. The mechanical instability induced by the direct touch could be the reason for the disappearance of the right sided hologram. Also the intensity of the irradiation from the magnetic body assignable to hand is expected to be stronger than the original reference beam so that the hologram is transformed to left-sided hologram. This explanation could be tested by touching the sample from another side to see whether the hologram remains right sided in this case.

2. One can imagine also alternative but more complex explanation not favored by Occam's razor. What comes in mind that the reference beam needed for the hologram and generated by DNA sample of the magnetic body is transformed to its unstable phase conjugate and thus travels from left to right and produces a left sided replica hologram. An open question is whether this hologram is from left hand side of the system or a mirror image of the hologram from right hand side. Perhaps this could be tested.

   DNA strands and their conjugates should correspond to separate flux sheets and one can wonder whether the double DNA strand maps to a doublet of magnetic bodies (note the analogy with two brain hemispheres and EEG) and whether left-right dichotomy could correspond to DNA-conjugate DNA dichotomy. If so, then touching would lead to the disappearance of DNA reference beam and the generation of its conjugate beam assignable to conjugate strand of DNA and perhaps scattering from the conjugate hologram also formed in the process.

4 The realization of the hologram at the level of magnetic body

How the reference beam is generated and how the hologram substrate is realized? These are the basic questions to be answered. Reference beam should be generated by the magnetic body itself and/or by DNA sample since it exists in absence of irradiation. Magnetic body should define the photosensitive substrate and the thickness of the analog of the photographic plate should be of the order of scaled up wavelength in order to achieve this. Note that in the case of EEG photons similar mechanism would mean that the size for the analog of the photographic plate is of order Earth size scale!

4.1 How the reference beams and reflected beams are generated?

The explanation for the replica assumes that the reflected beams are horizontal. Reference beams should be such that there exists a mechanism taking care the that they are preserved after the irradiations cease. The mechanism generating the reference beam would be most naturally the coherent decay of the excited state of a Bose-Einstein condensate. This condensate must be however assigned with some other structure than hologram substrate itself.

One can distinguish two DNA replica trajectories near DNA sample and there are even more of them at higher height (Fig. 3. The decay of the first replica trajectory could provide reference beam and reflected beam for the second replica trajectory acting as hologram substrate and vice versa. This

mechanism works for an arbitary number of hologram substrates and could be at work at red, IR, and UV wave lengths. The mechanism is actually the same as the one generating ordinary laser beams and skeptic can of course ask whether the large value of Planck constant is absolutely necessary.

The replica hologram obtained by method II involves several colors. The figures about the holograms show the presence of red light, reddish or white light, and also blue light and one must understand also this. Holograms are constructed using monochromatic laser light. The reading of the hologram is however possible using even white light if the reference beam is orthogonal to the hologram substrate since in the idealization that hologram is infinitely thin, the information about the wavelength of reference beam is completely lost in this case. The proposed model for the generation of reference is consistent with the orthogonality.

The picture that emerges would be following.

1. At least the incoming red beam is transformed after the passage through the sample to a beam with large value of Planck constant and wavelength of order say .2-.5 m corresponding to the size of the region appearing in the hologram. It is quite possible that also UV and IR photons transform to dark photons. At the magnetic flux tube this beam of dark photons is split to two pieces defining reference bream and the beam reflected from the objects of the environment. All these beams are nearly horizontal. The reflected beam and reference beam recombine and form a hologram substrate defined by magnetic flux tubes assigned to the DNA replica trajectory.

2. The cyclotron Bose-Einstein condensates at magnetic bodies function as analogs of lasers. Instead of the excitations of atomic states one has excitations of cyclotron states of a Bose-Einstein condensate with a large value of Planck constant. The excitation of these states requires pumping of energy. The simplest possibility is that both UV, IR, red, and IR light pump energy to the respective modes so that one would have multi-laser operation. The magnetic body is predicted to have a hierarchical fractal structure with magnetic fields whose strengths correspond to the p-adic length scale in question with p-adic length scales coming as half octaves of basic scale which conveniently can be taken 10 nm defining the thickness of cell membrane (for p-adic length scale hypothesis, which forms one of the corner stones of TGD based particle physics and of quantum biology see [12]. These irradiations would excite different parts of the magnetic body giving rise to a fractal hierarchy of holograms. The camera operating at visible wave lengths would not allow to see UV and IR holograms.

3. It is important to notice that the presence of only say red beam of light is not r enough to generate the hologram so that an interaction between these irradiations must be present. Some of the beams could act as control signals activating the DNA or as sources of metabolic energy (say UV beams).

4. The holograms appear periodically for method II [5]: Figs. 9, 10, 11, 12 at the end of the article illustrate what is involved. The periodic irradiation of the sample certainly induces a periodically appearing hologram image: when all irradiating beams are turned on, the conditions for the appearance of hologram are not satisfied and hologram disappears. The period is however considerably longer than the time interval between irradiation periods. This suggests a threshold for the effect.

   When the amount of pumped energy reaches a threshold, the intensity of the reference beam increases dramatically and the hologram becomes visible. This kind of effect requires a non-linear dynamics. The simplest model would be in terms of a potential containing the net value of the pumped energy as a parameter. As this parameter exceeds a threshold value, a phase transition the equilibrium position of the system would change from that with a vanishing reference beams to that with a large reference beam and the energy stored to the system would be utilized. DNA sample would be the natural storage of the energy.

4.2 A simple model for the dynamics of pumping and sustainment of dark photon beams

The basic question is what the pumping of energy could mean at the level of DNA. It seems clear that at least part of the pumped energy is transformed to metabolic energy in turn transformed to dark photons. It is also possible that the chemical energy of stored in DNA molecules is transformed

to metabolic energy. The existence of a hierarchy of universal metabolic energy quanta predicted by TGD provides the physical basis of the model.

One should also have a qualitative model for the transformation of the energy of radiation to metabolic energy and to the self sustainment of the dark photon beams.

1. The basic idea is simple. The irradiation kicks particles in DNA to higher energy state and these states decay to the ground state by emission of dark photons making allowing to realize the reference beam for holograms during reading period and both reflected and references beams during irradiation period.

2. For method I both the reference beam and reflected beam remain when irradiation ceases and give rise to the red phantom DNA replica (Fig. 5). For method II the presence of hologram image (Fig. 2) means that only reference beam is sustained. Self-sustainment requires non-linear dynamics. This dynamics could appear either at the level of DNA sample or at the level of the reference beam and reflected beams. For method II the white cable like structures appearing to the left of DNA sample could also correspond phantom DNA replica. They cannot however correspond to hologram like mechanism but ordinary radiation emitted by the hologram substrate.

3. The first possibility (option I) that the non-linear dynamics is realized at the level of DNA. DNA might be able to liberate chemical energy as metabolic energy or store the energy of irradiation and then liberate it. It is however difficult to understand why only the reference beam is sustained in method II. Both beams should be present if they result by a splitting of a beam coming from DNA meaning the absence of replica hologram. Internal consistency would require giving up hologram interpretation.

4. Second possibility (option II) is that non-linear dynamics is realized at the level of reference beam and reflected beams. For method II this dynamics could lead to a self sustainment in the case of reference beam if it is more intense than the reflected beams. For method I the irradiation lasts much longer and both reference beam and reflected beam could be sustained and one would not obtain hologram image but only phantom DNA replica image.

The following qualitative model has same general form for both options.

4.2.1 p-Adic length scale hypothesis and hierarchy of metabolic energy quanta

If one takes seriously the TGD inspired model for metabolic energy quanta, the irradiation would kick charged particles from larger space-time sheets to smaller ones so that the energy would go to the zero point kinetic energy plus surplus. The particles would drop back to the larger space-time sheets emitting the surplus zero point kinetic energy in this process as dark photon going to the magnetic flux tubes to be used to build reference beams and reflected beams for the holograms.

The kicked particles could be electrons or protons but electrons are more plausible candidates.

1. The nominal value of zero point kinetic energy given by

$$E_0 = \frac{3\hbar^2}{2mL^2} , \qquad (4.1)$$

and corresponds to zero point kinetic energy for a particle in box with side of length L.

2. Possible values of L can be estimated by assuming $L = L(k)$, with $L(k)$ given by the p-adic length scale hypothesis stating

$$L(k) = 2^{(k-151)/2} L(151) , \qquad (4.2)$$

where $L(151) \simeq 10$ nm corresponds to Gaussian Mersenne prime $M_{151,G} = (1+i)^{151} - 1$, which is one of the Gaussian Mersennes $M_{k,G}$, $k = 1151, 157, 163, 167$ between cell membrane thickness

10 nm and length scale 2.5 μm which is roughly one half of the size scale of cell nucleus. For $k = 148$ one obtains $E_0(148) \simeq .5$ eV which is the nominal value of metabolic energy quantum. Other zero point kinetic energies would come as octaves of $E_0(148)$ so that one has has the series (...,.25,.5,1,2, 4,..) eV. Nominal values are in question: the variation can be at least 10 per cent around the nominal value and is due to the fact that in reality space-time sheets do not have the geometry of cube and because the particles inside space-time sheets are not free.

3. Metabolic energy quanta correspond to the zero point kinetic energies liberated as particle drops from space-time sheet characterized by k_1 to $k_1 + \Delta k$ and are given as differences

$$\Delta E_0(k, k + \Delta k) = \frac{3\hbar^2}{2mL^2(151)} 2^{-k+151}(1 - 2^{-\Delta k}) \ . \qquad (4.3)$$

This gives a geometric series of metabolic energy quanta for each value of k. Two cases are of special interest: dropping next space-time sheet in the hierarchy ($\Delta k = 1$) and dropping to very large space-time ($\Delta k \to \infty$).

$$\Delta E_0(k, 1) = \frac{3\hbar^2}{2mL^2(151)} 2^{-k+151} \ ,$$
$$\Delta E_0(k, \infty) = \Delta E_0(k-1, 1) = \frac{3\hbar^2}{4mL^2(151)} 2^{-k+151} \ . \qquad (4.4)$$

4. Note that the energy levels form a cascade converging to $\Delta E_0(k, \infty) = \Delta E_0(k-1, 1)$. The scaling $\hbar = r\hbar_0$ of Planck constant does not affect the spectrum of metabolic energy quanta if L(k) scales as $L(k) \to rL(k)$.

5. The following table lists the three p-adic length scales, which are possible for the radiation sources used assuming that $\Delta k = 1$ transitions dominate.

k	145	144	143
$\Delta E_0(k, 1)$/ eV	2	4	8
λ/ nm	620	310	155
L(k)/ nm	1.23	.88	.625

(4.5)

The 2 eV metabolic energy is five percent larger than the energy 1.91 eV assignable to 650 nm wavelength of the red light used in irradiation. These wave lengths would be preferred but in principle entire range of metabolic energy quanta is allowed and if one assigns metabolic energy quanta to the transitions $\Delta k \to \infty$ the values of k in the equation are scaled down by one unit: $k \to k - 1$. The p-adic length scales correspond to length scales naturally associated with DNA.

In the case of proton the length scales would be obtained by the replacement $k \to k - 11$ and would be considerably below the atomic length scale L(137) for the ordinary value of Planck constant and dark protons would be required.

4.2.2 Linear model for the pumping of energy

If one assumes that the non-linear behavior responsible for self-sustainment is realize at the level of the reference beams and reflected beams the model for pumping of energy to DNA sample can assumed to be linear. The simplest model for the pumping involves only two space-time sheets. The proper variable would be either the number N of charged particles -presumably electrons- and/or net zero point kinetic energy feed to the smaller space-time sheet. One has just population dynamics for the numbers of electrons at the two space-time sheets involved.

1. The equations for the population dynamics have the general form

$$\begin{aligned} \frac{dN_1}{dt} &= k_0(t)N_2 - k_1(t)N \ , \\ \frac{dN_2}{dt} &= -k_0(t)N_2 + k_1(t)N \ , \end{aligned} \tag{4.6}$$

The first term on the right hand side corresponds to the energy feed from irradiation and second term the energy leakage through the dropping of the particles back to the smaller space-time sheet.

2. If the N_2 is very large it can be taken as constant not affected by the process and with an obvious redefinition of $k_0(t)$ one can write

$$\frac{dN_1}{dt} = k_0(t) - k_1(t)N_1 \ . \tag{4.7}$$

The general solution of the equation is

$$N_1(t) = N_0 \exp(-\int k_1 dt) + \int_0 N_1 \exp(\int_0 k_1 dt) k_0(t) dt \ . \tag{4.8}$$

As noticed, this model cannot explain self-sustainment in terms of metabolism.

4.2.3 A catastrophe theoretic model for the self-sustainment

The self-sustainment of the beams requires non-linear dynamics. The non-linearity could be assigned with the pumping of energy to DNA by irradiation and would mean the addition of non-linear terms to the population dynamics of electrons (Eq. 4.7). This model does not however allow to distinguish between reference beams and reflected beams. The same formal model however applies also to the dark reference beams and reflected beams by re-interpreting number N of electrons as the number of photons in the beam. The following model is only an attempt to characterize the situation qualitatively and does not depend on the interpretation of N. The two alternative interpretations will be referred to as options I and II.

1. The basic equation is

$$\frac{dN}{dt} = P_3(N, k_0) = k_0(t) - k_1(t)N + k_2(t)N^2 - k_3(t)N^3 \ . \tag{4.9}$$

The parameters $k_i(t)$ are assumed to be slowly varying in the time scale of the dynamics for N. In catastrophe theoretic setting [1] k_i resp. N would be called control parameters resp. behavior variable. Depending on option N denotes either the number of electrons kicked to a smaller space-time sheet of photons in the analog of laser beam.

   (a) For option I $k_0(t)$ characterizes the rate at which the irradiation kicks electrons to the smaller space-time sheet. For option II the interpretation is as a rate with which photons in the dark analog of laser beam are produced by irradiation. One can assume that $k_0(t)$ is constant during periods of irradiation and is small and vanishes when there is no irradiation.

$$\begin{aligned} k_0(t) &= k_0 \text{ during irradiation} \ , \\ k_0(t) &= 0 \text{ in absence of irradiation} \ . \end{aligned} \tag{4.10}$$

(b) For option I the term $-k_1N_1$ corresponds to the dropping of the electrons back to the large space-time sheets. For option II it corresponds to the leakage and absorption of photons from the beam.

(c) For option I the presence of k_2N^2 can make possible self-sustained metabolism and therefore also that of dark photon beams. DNA itself can somehow kick the electrons to smaller space-time sheets. This could be due to the liberation of metabolic energy from DNA, which cannot continue indefinitely so that $k_2(t)$ must go to zero in some time scale of the order of the time period between successive shots (few seconds). For option II this term correspond to non-linear self-amplifying interaction of laser beams and could be due to a resonant interaction of beams associated with different parts of the magnetic body.

(d) The term $-k_3N^3$ is necessary in order to avoid endlessly increasing N, which is definitely something non-realistic.

2. By construction the system realizes cusp catastrophe [1] describing the simplest possible situation in which some parameter region of parameter space allow 3 or only 1 root to the stationarity condition $P_3(N,k_0) = 0$ so that one has a phase transition like behavior. The following considerations show that if $P_3(N,0)$ allows three non-negative roots and $P_3(N,k_0)$ only one positive root, then sufficiently many and sufficiently long irradiation periods allow to achieve a self-sustaining situation, which lasts as long as $k_2(t)$ characterizing self-sustainment remains large enough. After this a phase transition to a phase characterized by a rapid decrease of N, occurs.

3. One can concretize the situation by imagining that the system climbs to a mountain during the irradiation periods and slides down when the irradiation is off in the case that one has

$$R \equiv \lim_{t \to t_f,+} dN/dt(t) = P_3(N(t_f),0) < 0 \ . \tag{4.11}$$

Here t_f denotes the value of time when irradiation ends. For $R > 0$ the climbing up continues spontaneously but with a slower rate.

4. Quite generally, $P_3(N,k_0)$ can have $n = 0,1$ or $n = 3$ zeros in the region $N \geq 0$. $P_3(N,0)$ has always zero at origin and can have two additional zeros of $k_2(t)$ is large enough. Since the polynomials $P_3(N,k_0)$ and $P_3(N,0)$ differ only by a downwards shift by k_0, one finds the following.

(a) If one has

$$P_3(N,k_0) < k_0 \tag{4.12}$$

for $N > 0$, $P_3(N,0)$ has only one non-negative zero for all positive values of N. The system slides dow towards $N = 0$ as the irradiation ceases.

(b) If the condition

$$P_3(N_f,k_0) \geq k_0 \tag{4.13}$$

is satisfied, $P_3(N_f,0)$ has two positive roots $(N_{2,0},N_{3,0})$ besides $N_{1,0} = 0$. If R is in the region above $N_{2,0}$, the system slides down to or climbs up to $N_{3,0}$ after the irradiation has ceased. This situation is obviously the interesting one in the recent case. Whether the region $N > N_{2,0}$ can be reached during irradiation depends on the properties of $P_3(N,k_0)$.

5. Consider first what happens during irradiation assuming that $P_3(N_f,0)$ has two positive roots $(N_{2,0},N_{3,0})$ besides $N_{1,0} = 0$ (the interesting case). $P_3(N,k_0)$ has certainly one root since $P_3(N,f)$ becomes eventually negative due to the term $-k_3N^3$.

(a) If k_0 is large enough there is only one root - call it N_3. One has $N_3 > N_{3,0}$ and the energy feed - if allowed to continue long enough or for sufficiently many times- drives the system above $N_{2,0}$ and eventually to N_3, which is stable and is reduced only slowly as $k_2(t)$ decreases. When irradiation ceases, the system goes to $N_{2,0}$, which represents a stable situation and only adiabatically approaches to zero as long as the number of roots remains three. After this N goes rapidly to zero.

(b) If k_0 is small enough one has one or three roots- let the three roots be $N_1 < N_2 < N_3$. N_1 corresponds to a stable situation in which the linear term has driven dN/dt to zero. One ends up to this situation either from $N \leq N_2$ for three roots and always if one has only one root. Only N_1 is achievable by starting from $N(t = 0) = 0$ or from $N(t_f)$ achievable during irradiation period. Since the graphs of $P_3(N, k_0)$ and $P_3(N, 0)$ differ only by a shift, it is clear that one has $N_1 < N_{2,0}$ so that the system rapidly slides down to $N = 0$.

6. The conclusion is that the desired situation can be achieved only if $k_2(t)$ is so large that $P_3(N, k_0) > k_0$ holds true at the maximum of $P_3(N, k_0)$ (for $N > 0$) and k_0 is so large that $P_3(N, k_0)$ has only single root. This means that the minimum of $P_3(N, k_0)$ is positive. The extrema $N_\pm$ of $P_3(N, k_0)$ correspond to the vanishing of $dP_3(N, k_0)/dN$ so that one has

$$\begin{aligned} N_\pm &= \frac{k_2}{3k_3} \pm \sqrt{(\frac{k_2}{3k_3})^2 - \frac{k_1}{3k_3}}\ , \\ (\frac{k_2}{3k_3})^2 - \frac{k_1}{3k_3} &\geq 0\ , \end{aligned} \tag{4.14}$$

The conditions for self-sustainment boil down to the equations

$$\begin{aligned} P_3(N_+, 0) &> 0\ , \\ P_3(N_-, k_0) &> 0\ . \end{aligned} \tag{4.15}$$

Self-sustaining situation continues as long as $k_2(t)$ is so large that one has 3 roots for $P_3(N, 0)$. For small enough $k_2(t)$ the two roots disappear and the system slides rapidly to $N = 0$. Fig. 1 illustrates these conditions graphically.

4.3 A general model for the hologram substrate

The following model for the hologram substrate is based on the earlier vision about the role of Bose-Einstein condensates of Cooper pairs and bosonic ions in TGD inspired quantum biology.

1. DNA replica trajectory should define the analog of the photosensitive substrate so that the scaled up wave length defining its thickness should be of order 1 cm. The TGD inspired model for the effects of ELF em fields on vertebrate brain [31] leads to the proposal that Bose-Einstein condensates of various biologically important ions and of Cooper pairs of electrons in the magnetic field associated with the flux quantum define a key element of biological information processing.

   The natural guess is that this process involves in an essential manner the formation of holograms by a radiation generating cyclotron transitions and in this manner affecting the reflective properties of the hologram substrate determined by the rates of elastic scattering. If the flux quanta are flux tubes, one has photo-sensitive tubes instead of photosensitive plates and only the vertical component of the photon momentum is conserved in the scattering and reflected photons can have any direction in the plane orthogonal to the flux tube so that the reflected radiation indeed reaches camera. The properties of the hologram seem to be consistent with the prediction that the information carried by it is only about the vertical and preferred horizontal direction.

2. Cyclotron energies E_c are proportional to $\hbar eB/m$ so that they increase with Planck constant and are inversely proportional the mass of the charged particle. This selects the Cooper pairs of electrons as a unique candidate for the Bose-Einstein condensate. TGD assigns to elementary particles macroscopic time scales as fundamental time scales and in the case of electron this time scale is .1 seconds which corresponds to 10 Hz fundamental biorhythm. Also for this reason Bose-Einstein condensate of Cooper pairs of electrons defines a natural candidate for the hologram substrate.

3. Cyclotron transitions induced by the incoming dark photons should in the recent case have frequency of order 30 GHz if $\lambda_d \sim 1$ cm is assumed for the dark variant of red light. In the case of electron the magnetic field .2 Gauss (this is the value of endogenous magnetic field deducible from the effects of ELF em fields on vertebrate brain [31, 15]) corresponds to frequency of about 6×10^5 Hz so that a magnetic field of order .1 Tesla would give rise to a cyclotron frequency of order 30 GHz. The corresponding magnetic length is $L_B = \sqrt{\hbar/eB}$, which for ordinary value of Planck constant is 4.7×10 nm (note that 10 nm corresponds to cell membrane thickness and thickness of chromosomes). For $r = 15 \times 10^3$ the magnetic length would correspond to 5.8μm length scale to be compared with the size scale 6 μm of cell nucleus. If one requires the quantization of magnetic flux in multiples of $\hbar$ this field corresponds flux tube with thickness of order 6 μm. Therefore there might be a connection with the size of nucleus and the quantization of magnetic flux meaning that the thickness of the DNA replica trajectory reflects the basic cellular length scales.

4. The cyclotron states of Cooper pairs are harmonic oscillator states in the radial direction of flux tube and eigen states of angular momentum and momentum in the direction of the flux tube labelled by (n, m, k). The integer n is harmonic oscillator quantum number. m and k characterize the projections of angular momentum and momentum in the direction of the flux tube. m is integer and also k is quantized from periodic boundary conditions for the flux tube.

5. The hologram would be generated when the incoming dark photons excite Cooper pairs from the lowest energy eigenstate with oscillator quantum number $n = 0$ to the first eigenstate with $n = 1$ and in this manner affect the reflection properties of the system. The life-time of the hologram is determined by the rate at which the system decays back to the ground state so that one would have dynamical rather than static hologram which is of course what biological system needs.

6. The reflection from the hologram corresponds to an elastic scattering in which the Cooper pair condensate receives momentum but its energy is not affected. Elasticity means that the transition does not affect the energy of the Cooper pair which is the sum

$$E_{n,m,k} = n\hbar\omega + \frac{\hbar^2 k^2}{2m}$$

of the cyclotron energy and kinetic energy of free motion in the direction of the flux tube. If the longitudinal momentum k vanishes as the formation mechanism of the hologram strongly suggests, the value of n remains unchanged but the value of angular momentum projection m in the direction of flux tube can change in elastic scattering. The scattering takes place coherently so that the rate is proportional to N^2, N the number of Cooper pairs. The rate of these transitions is affected when a position dependent portion of the Cooper pairs of the Bose-Einstein condensate is in higher energy state. Therefore the transmittance depends on the point of hologram and the change is in the lowest approximation proportional to the intensity $|A + A_R|^2$ of the incoming dark light as in the case of the ordinary hologram.

4.4 Is the lifetime of the hologram long enough?

The lower bound for the lifetime of the physical realization of the hologram must be measured in seconds from the results of method II. The lifetime can be also longer since the fading of the physical hologram after the irradiation has ceased can be due do the decay of the reference bream. This means a killer test for the model since the decay rate of the hologram is easy to estimate. The decay rate of hologram can be estimated from the decay rate of excited cyclotron state and the calculation

reduces to standard first order perturbation theory for interacting system of charged particles and electromagnetic field which can be found in text books [2].

1. The lifetime of the hologram can be estimated as the life-time of the excited state. The excited state decays by a spontaneous emission of photons. The lifetime can be estimated by using standard perturbation theory for the interaction of radiation fields and electrons with a scaled up value of Planck constant. Electrons form cyclotron states at flux tubes characterized by three quantum numbers: the harmonic oscillator quantum number $n = 0, 1, 2..$, the angular momentum projection m in the direction of flux tube, and the momentum of electron in the direction of flux tube.

   The interaction Hamiltonian is obtained by the minimal coupling prescription by adding to the vector potential associated with the static magnetic field of the flux tube time dependent radiation part. This means the replacement

   $$A = A_{flux} \to A_{flux} + A_{rad} \tag{4.16}$$

   of the vector potential of the static magnetic field determining cyclotron energy spectrum in the magnetic field parallel to the flux tube with a vector potential containing also the vector potential of the second quantized radiation field.

2. This replacement affects the Hamiltonian of the system in the following manner

   $$\begin{aligned} H_0 &= \frac{1}{2m}(p - ZeA_{flux}) \cdot (p - Ze(A_{flux}) \to H \ , \\ H &\equiv H_0 + H_{int} = \frac{1}{2m}(p - Ze(A_{flux} + A_{rad})) \cdot (p - Ze(A_{flux} + A_{rad})) \ , \\ H_{int} &= -\frac{1}{2m}\left(Zep \cdot A_{rad} + A_{rad} \cdot p) + Z^2e^2A_{flux} \cdot A_{rad} + Z^2e^2A_{rad} \cdot A_{rad}\right) . \end{aligned} \tag{4.17}$$

   $Z = 2$ is the charge of the electron Cooper pair and $m = 2m_e$ is its mass. In Coulomb gauge one has

   $$\nabla \cdot A_{rad} = 0$$

   and the the interaction Hamiltonian H_{int} determining the transition rate reduces in the lowest order to

   $$\begin{aligned} H_{int} &= -\frac{Ze}{m}A_{rad} \cdot p \ , \\ p &\equiv \frac{\hbar}{i}\nabla \ . \end{aligned} \tag{4.18}$$

3. If the radiation generating hologram is in horizontal plane, cyclotron states have vanishing momentum quantum number in the vertical direction. Therefore also the emitted radiation has momentum and polarization in this plane. In principle this could be tested by using polarization sensitive camera.

4. The rate for the return to the ground state is calculable by using standard time dependent perturbation theory the result of which can be expressed as a formula for the total transition rate to the ground state

   $$\Gamma = \frac{mE}{(2\pi)^2\hbar^4}\int d\Omega |\langle f, \hbar k | H_{int} | i \rangle|^2 \ . \tag{4.19}$$

   Here integration is over the solid angle that is over the momentum directions of the emitted photon. Here m is the mass of Cooper pair (two times electron mass) and E is photon energy (in eV range for visible photons).

5. The matrix element $|\langle f,\Box k|H_{int}|i\rangle$ of the interaction Hamiltonian is expressible in the lowest order approximation as

$$\langle f,\Box k|H_{int}|i\rangle = -i\frac{\Box Ze}{m\sqrt{\bar{\omega}}}\int \bar{\Psi}_{n_f,m_f,k_f}e^{ik\cdot r}e\cdot\nabla\Psi_{n_i,m_i,k_i}dV \quad . \tag{4.20}$$

e denotes the polarization vector of the photon and k its wave vector. The integration is over the flux tube volume.

In dipole approximation one can expand the plane wave to the first non-trivial order. If one assumes that the transitions responsible for the decay of the hologram correspond to the transitions $(n_i,m_i,0)=(1,\pm 1,0)\rightarrow(n_f,m_f,0)=(0,0,0)$, one has

$$\langle f,\Box k|H_{int}|i\rangle \Box \frac{\Box Ze}{m\sqrt{\bar{\omega}}}\int \bar{\Psi}_{0,0,0}e\cdot\nabla\Psi_{1,\pm 1,0}dV \quad . \tag{4.21}$$

The result does not depend on photon energy at all. Angular momentum conservation requires that the angular momentum projection of the state in the direction of the flux tube changes by one unit corresponding to the spin of the photon. This allows to transform the matrix element to

$$\langle f,\Box k|H_{int}|i\rangle \Box \pm i\frac{\Box Ze}{m\sqrt{\bar{\omega}}}\int \bar{\Psi}_{0,0,0}e\times e_\rho\frac{1}{\rho}\Psi_{1,\pm 1,0}dV \quad . \tag{4.22}$$

Here e_ρ denote the unit vector $(xi+yj)/\rho$ in radial direction. The magnitude of the matrix element is of order

$$\langle H_{int}\rangle \sim (\Box Ze/m\sqrt{\bar{\omega}})\times\langle\frac{1}{\rho}\rangle\sim\frac{\Box e}{mR\sqrt{\bar{\omega}}} \quad , \tag{4.23}$$

where R is the radius of the flux tube.

6. The overall rate for the decay of the hologram has the order of magnitude

$$\Gamma \sim \frac{4\pi^2\alpha}{r}\frac{\Box_0}{R^2m_e}\sim\frac{4\pi^2\alpha}{r^3}\frac{\Box_0}{\lambda^2m_e} \quad , \quad r=\frac{\Box}{\Box_0} \quad . \tag{4.24}$$

Here λ denotes the wave length of ordinary visible photon. Formally the rate scales as $1/r$ as the naive dimensional estimate suggests but $R\Box r\lambda$ brings in an additional $1/r^2$ reduction factor so that $1/r^3$ over-all dependence results. For $r=\Box/\Box_0\sim 10^4$ the order of magnitude for the decay rate is for visible light $\Gamma\sim 10^{-5}\ s^{-1}$, which is consistent with the observed slow rate of decay. As noticed, the fading of the hologram in experiment two could be due to the decay of the reference beam rather than the decay of hologram. Maybe also this could be tested. In any case, the model survives the first killer test.

4.5 The amplitude for the elastic scattering from hologram

The rate for the elastic scattering of photons of the reference beam from the hologram substrate defines the intensity of the hologram image and should be high enough.

1. This process involves two photons. The term

$$H_{int}^{2)}=\frac{e^2}{2m}A_{rad}\cdot A_{rad} \tag{4.25}$$

in H_{int} makes this transition possible in the first order of perturbation theory.

2. One can worry about second order perturbation theoretic contribution to the rate which is also of order e^2. The generalization of the Golden Rule is obtained by the replacement

$$\langle f|H_{int}|i\rangle \;\rightarrow\; \langle f|H_{int}|i\rangle + \sum_m \frac{\langle f|H_{int}|m\rangle\langle m|H_{int}|i\rangle}{E_n - E_0 + i\eta} \quad , \quad \eta \rightarrow 0_+ \quad . \tag{4.26}$$

The sum over m denotes sum over intermediate states. In the second order of perturbation theory the scattering can be thought of as taking place via intermediate states of Cooper pairs decaying back to the original state via the emission of photon. In the following rough estimate only the lowest ordinary contribution is taken into account.

3. In this approximation the amplitude for elastic scattering responsible for the hologram formation with $(n_i, m_i, k_i) = (n_f, m_f, k_f)$ and $\omega_i = \omega_f = \omega$ with the amplitude is apart from numerical factor of order unity given by

$$\langle f, k|H_{int}|i\rangle \;=\; \frac{e^{2}\hbar^{1/2}e_i \cdot e_f\,\omega}{m\sqrt{\omega_f}} \int \overline{\Psi}_{n_i,m_i,0}e^{i(k_i - k_f)\cdot r}\Psi_{n_i,m_i,0}dV \quad . \tag{4.27}$$

In the lowest order approximation plane wave factor can be neglected. The order of magnitude for rate differs by a factor $4\pi\alpha(\omega R)^2$ from the matrix element for the decay of the hologram. For $R \sim \lambda_d$ the rates are of the same order. This rate corresponds to single photon case. In the case of many-photon state defined by the reference beam the rate is amplified by a factor N^2, where N is the number of photons in the reference beam.

5 Appendix: Details about methods I and II

Methods two represent the two schemes developed for our experimental purposes. In order to adduce and visualize DNA wave replicas, the following is to be performed: by means of timing relay (Fig. 13, position # 3) in varied combinations the operator switches on the required emitters BS (UV-B, which is incandescent lamp in blue spectrum, glass type- Fig. 13, position # 5), a matrix with red and infrared diodes (Fig. 13, position # 8) and germicidal mercurial lamp/ bulb or lamp Compact electronic CEST 26E27 Black (UV-C, Fig. 13, position # 6), or BS (UV-B) and MXT-90 (cold cathode Fig. 13, position # 4).

1. Method I.
   Dehydrated/ dry DNA sample from bull' s spleen - about 100 milligrams in a sealed plastic conical test tube, which is 4 centimeters long and 0.9 cm in its upper end; or 3 milliliters of DNA water solution, 1mg/ ml) are placed in the effective zone of the emitters (1mm-50cm from the light emitters) and then the emitters are activated. The progression of the experiment was filmed using Fuji 24-27 DIN film. Oscillograph is in operation during the experiment and is to register and record the electromagnetic fields/ frequencies within the zone of the experiment; averaged normal electromagnetic background noise from within the premises is recorded, defined by the behavior of sinusoid in the oscillograph. Further, by means of the timing relay the emitter UV-C is turned off 10 minutes later. The camera captures an emergence of unique dynamic wave structures multi-replicated DNA replicas and of the surrounding objects invisible to the naked eye, yet perceivable by the camera and fixed on the film. These are directly related to the photonic influences effected by the emitters on the DNA samples. In other words, multiplication of a number of reflection of DNA samples occurs and is redistributed in space on complex trajectory patterns (the first method) and on horizontal patterns (the second method), including mapping of the objects responsible for exciting the DNA samples.

2. Method II
   The second method to obtain and visualize DNA wave replicas involves the following: dehydrated/ dry DNA sample, 100 milligrams is placed in an open mode into a holder made of aluminum foil. With intervals of 2-3 seconds the BS (UV-B) lamp, Compact Electronic CEST 26E27

Black lamp and apparatus Duna-M are turned on and off. Photographs are taken 5 minutes later. By this method the DNA replicas and of close objects are registered and they are propagating strictly to the right hand side. With external mechanical interference (a touch3) with the DNA samples the distribution vector alters to the opposite that is the DNA replicas begin propagating to the left hand side and than 5-8 seconds after the mechanical interference the replicas disappear or are not perceived by the present equipment4 or the utilized film, regardless of the equipment still being in an activated state.

References

General references

[1] E. C. Zeeman (ed.)(1977), Catastrophe Theory. Addison-Wessley Publishing Company.

[2] G. Baym (1969), Lectures on Quantum Mechanics, W. A. Benjamin, Inc..

[3] P. P. Gariaev, V. I. Chudin, G. G. Komissarov, A. A. Berezin , A. A. Vasiliev (1991), Holographic Associative Memory of Biological Systems. Proceedings SPIE - The International Society for Optical Engineering. Optical Memory and Neural Networks. v.1621, p. 280- 291. USA.

[4] P. Gariaev et al (2000), The DNA-wave-biocomputer. CASYS'2000, Fourth International Conference on Computing Anticipatory Systems, Liege, 2000. Abstract Book, Ed. M. Dubois.

[5] P. P. Gariaev, G. G. Tertishni, A. V. Tovmash (2007), Experimental investigation in vitro of holographic mapping and holographic transposition of DNA in conjuction with the information pool encircling DNA. New Medical Tehcnologies, # 9, pp. 42-53. The article is in Russian but Peter Gariaev kindly provided a translation of the article to English.

[6] P. P. Gariaev et al(2002), The spectroscopy of bio-photons in non-local genetic regulation. Journal of Non-Locality and Remote Mental Interactions, Vol 1, Nr 3. http://www.emergentmind.org/gariaevI3.htm.

[7] F. A. Popp, B.Ruth, W.Bahr, J. Boehm, P.Grass (1981), G.Grolig, M.Rattemeyer, H.G.Schmidt and P.Wulle: Emission of Visible and Ultraviolet Radiation by Active Biological Systems. Collective Phenomena(Gordon and Breach), 3, 187-214.
F. A. Popp, K. H. Li, and Q. Gu (eds.) (1992): Recent Advances in Bio-photon Research and its Applications. World Scientific, Singapore-New Jersey.
F.- A. Popp: Photon-storage in biological systems, in: Electromagnetic Bio-Information. pp.123-149. Eds. F.A.Popp, G.Becker, W.L.König, and W.Peschka. Urban & Schwarzenberg, Muenchen-Baltimore.
F.-A. Popp (2001), About the Coherence of Bio-photons.
http://www.datadiwan.de/iib/ib0201e1.htm.
F.-A. Popp and J.-J. Chang (2001), Photon Sucking and the Basis of Biological Organization. http://www.datadiwan.de/iib/ib0201e3.htm.
F.-A. Popp and Y. Yan (2001), Delayed Luminescence of Biological Systems in Terms of States. http://www.datadiwan.de/iib/pub2001-07.htm.

[8] J. Benveniste et al (1988). Human basophil degranulation triggered by very dilute antiserum against IgE. Nature 333:816-818.

[9] J. Benveniste et al (198?). Transatlantic transfer of digitized antigen signal by telephone link. Journal of Allergy and Clinical Immunology. 99:S175 (abs.). For recent work about digital biology and further references about the work of Benveniste and collaborators see http://www.digibio-.com/.

[10] L. Montagnier, J. Aissa, S. Ferris, J.-L. Montagnier, and C. Lavall'e (2009). Electromagnetic Signals Are Produced by Aqueous Nanostructures Derived from Bacterial DNA Sequences. Interdiscip. Sci. Comput. Life Sci.. http://www.springerlink.com/content/0557v31188m3766x/.

[11] J. B. Pawley (1990) In Handbook of Biological Confocal Microscopy (J. B. Pawley, ed.), 2nd Ed., p. 84. http://html-pdf-converter.com/pdf/handbook-of-biological-confocal.html.

[12] M. Pitkänen (2010), Article series about Topological Geometrodynamics in Prespacetime Journal Vol 1, Issue 4. http://www.prespacetime.com/file/PSTJ_V1(4).pdf.

[13] M. Pitkänen (2010), TGD Inspired Theory of Consciousness. Journal of Consciousness Exploration & Research, March 2010, Vol. 1, Issue 2, pp. 135-152. http://www.jcer.com/file/JCER_V1(2).pdf.

[14] M. Pitkänen (2010), Quantum Mind in TGD Universe, Journal of of Consciousness Exploration & Research— November 2010, Vol 1, Issue 8, pp. 971-991. Quantum Dream Inc.. http://www.jcer.com/file/JCER_V1(8).pdf.

[15] M. Pitkänen (2010), Quantum Mind, Magnetic Body, and Biological Body, Journal of of Consciousness Exploration & Research, November 2010, Vol 1, Issue 8, pp. pp. 992-1026. Quantum Dream Inc.. http://www.jcer.com/file/JCER_V1(8).pdf.

[16] Alexander Gurwitsch. http://en.wikipedia.org/wiki/Alexander_Gurwitsch.

[17] Alfven wave. http://en.wikipedia.org/wiki/Alfvn_wave.

References to books about TGD and TGD Inspired Theory of Consciousness and Quantum Biology

[18] M. Pitkänen (2006), Quantum TGD.
http://tgd.wippiespace.com/public_html/tgdquant/tgdquant.html.

[19] M. Pitkänen (2006), Quantum Hardware of Living Matter.
http://tgd.wippiespace.com/public_html/bioware/bioware.html.

[20] M. Pitkänen (2006), Genes and Memes.
http://tgd.wippiespace.com/public_html/genememe/genememe.html.

[21] M. Pitkänen (2006), Bio-Systems as Conscious Holograms.
http://tgd.wippiespace.com/public_html/hologram/hologram.html.

[22] M. Pitkänen (2006), TGD and EEG.
http://tgd.wippiespace.com/public_html/tgdeeg/tgdeeg.html.

[23] The chapter Does TGD Predict the Spectrum of Planck Constants? of [18].
http://tgd.wippiespace.com/public_html/tgdquant/tgdquant.html#Planck.

[24] The chapter DNA as Topological Quantum Computer of [20].
http://tgd.wippiespace.com/public_html/genememe/genememe.html#dnatqc.

[25] The chapter Three new physics realizations of the genetic code and the role of dark matter in bio-systems of [20].
http://tgd.wippiespace.com/public_html/genememe/genememe.html#dnatqccodes.

[26] The chapter The Notion of Wave-Genome and DNA as Topological Quantum Computer of [20].
http://tgd.wippiespace.com/public_html/genememe/genememe.html#gari.

[27] The chapter Quantum Antenna Hypothesis of [19].
http://tgd.wippiespace.com/public_html/bioware/bioware.html#tubuc.

[28] The chapter Bio-Systems as Conscious Holograms of [21].
http://tgd.wippiespace.com/public_html/hologram/hologram.html#hologram.

[29] The chapter Homeopathy in Many-Sheeted Space-Time of [21].
http://tgd.wippiespace.com/public_html/hologram/hologram.html#homeoc.

[30] The chapter Magnetic Sensory Canvas Hypothesis of [22].
http://tgd.wippiespace.com/public_html//tgdeeg/tgdeeg/tgdeeg.html#mec.

[31] The chapter Dark Matter Hierarchy and Hierarchy of EEGs of [22].
http://tgd.wippiespace.com/public_html/tgdeeg/tgdeeg.html#eegdark.

6 Figures

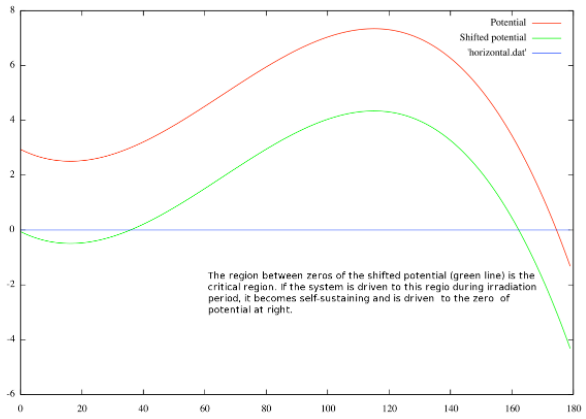

Figure 1: Illustrations of a potential $V(x) = P_3(x) = a - bx + cx^2 - dx^3$ and shifted potential $V(x) - a$ allowing self-sustainment. Note that the full potential allows only single zero and shifted potential two zeros. If the system ends up to the region between the two zeros of the shifted potential during irradiation, it ends up to the the rightmost zero after the irradiation period. When the value of the parameter c decreases adiabatically below certain critical value, the value of x (having interpretation as photon number) goes rapidly to zero.

Figure 2: The left hand side figure is from [28] and represents the replica images of the instruments and the image interpreted by experimenters as a replica image of DNA sample (method II). The white cable like structures to the left from DNA sample have interpretation as phantom DNA image.

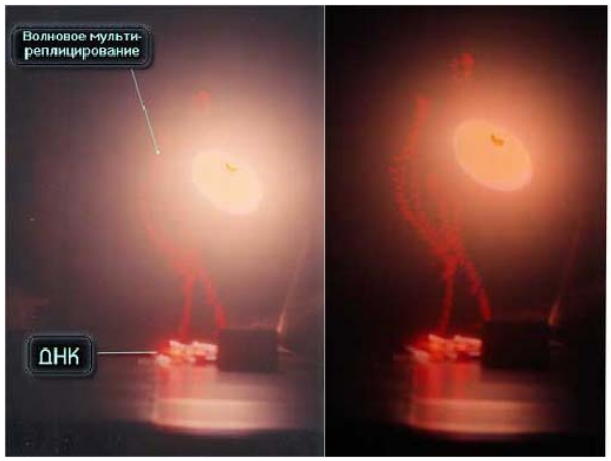

Figure 3: The picture shows the discrete replica like structure of the band like image obtained by method I and interpreted by experimenters as replica image of DNA sample.To the left image is the original image and to the right the contrasted one.

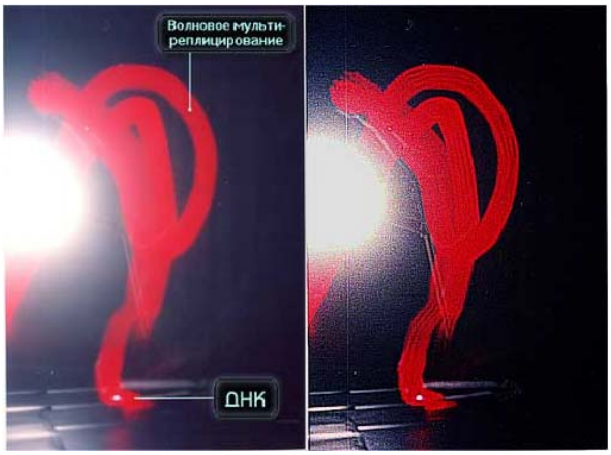

Figure 4: Spatial structure of DNA wave replicas obtained by method I. The picture reveals the 5-fold fine structure of the tube like image interpreted by experimenters as replica image of DNA sample. The 5-fold character probably correspond to five red LEDs above the sample. To the left image is the original image and to the right the contrasted one.

Figure 5: Long living DNA wave replica from the experiment in Fig. 3 (referred to as phantom image as opposed to the image seen during irradiation) subsequent to switching off of the initiating electromagnetic fields/ frequencies sources.

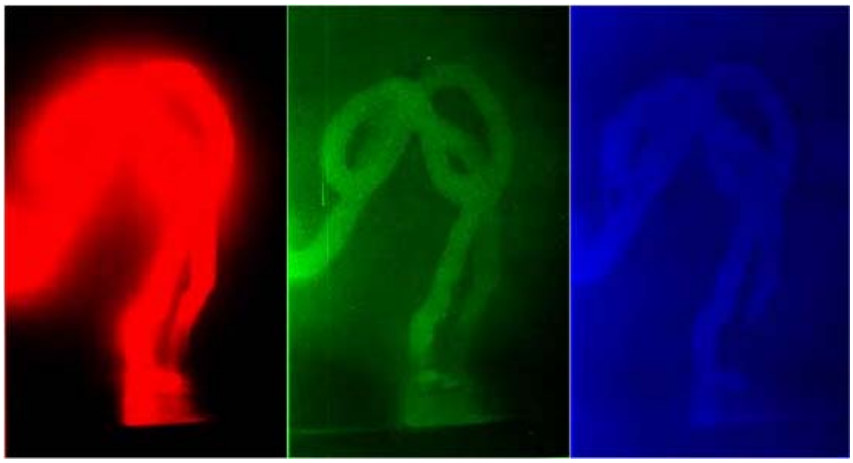

Figure 6: Distribution of the brightness values per RGB color model, Red, Green, Blue of the phantom DNA image of previous figure. The green image gives especially clear picture about the structure of phanton DNA image.

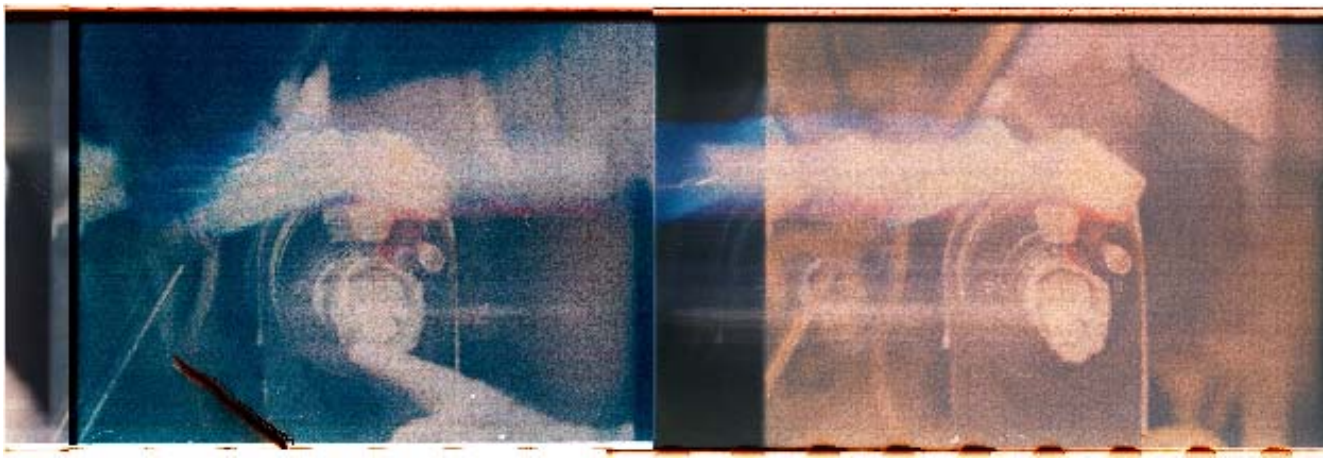

Figure 7: a) The moment of mechanical external interference (touch, which could have also biological effect) with DNA sample. The second method of elicitation of DNA wave replicas. b) Shift to the left of the wave replicas immediately after the interference. It is also commonly noticed that there is a sharp distinction of the shot from others by brightness and color scheme, which is unrelated to the working of the camera.

Figure 8: Disappearance of DNA wave replica formation effect after 5-8 seconds following the interference with the DNA sample (touch, see previous figure) while the entire equipment initializing the replicas is still on.

Figure 9: One of the modified experiments, shown in Fig. 5 (old DNA sample replaced by new). Refer to the shots # 3 and # 4 above. The shot # 4 reveals replicas of the Duna-M diodes, shifting to the right side. Note the appearance of replicas of perforation and exposed parts of the film close to diodes.

Figure 10: Shots # 11 and # 12 above. It is to be mentioned that from shot # 1 until shot # 11 the Duna-M diodes wave replicas are absent, however appearing again in the shot # 12.

Figure 11: Shots # 13 and # 14 above. In the # 13 we can distinguish wave replicas of the Duna-M diodes with the commonly observed intrusion in into the unexpected space between the shots. The shot # 14 does not capture the wave replicas of the diodes and they disappear.

Figure 12: Shots # 23 and # 24 above. From shot # 14 until # 22 replicas disappear, they are dimly captured in the shots # 23 and # 24.

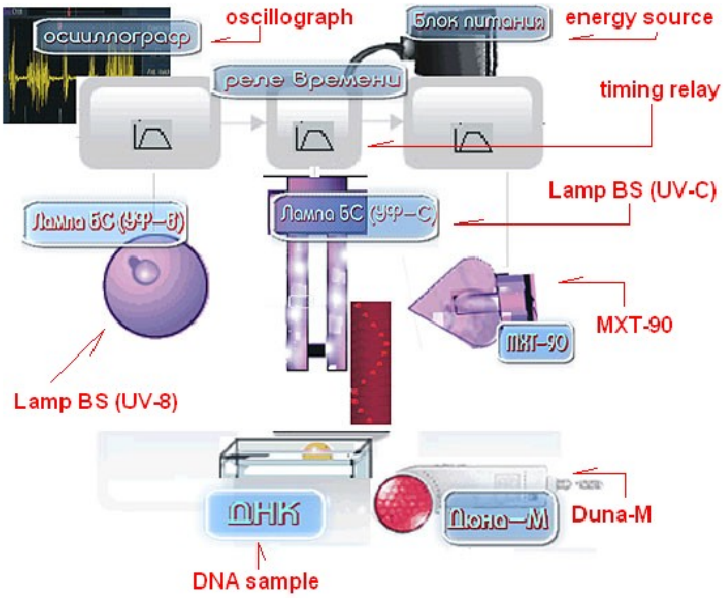

Figure 13: Schematic representation of the parts of the experimental apparatus